Higher performances of open vs. closed circuit microbial fuel cell sensor for nitrate monitoring in water

Zhenxing Ren, Guixia Ji, Hongbo Liu, Ping Li, Jianhong Huang, Eric Lichtfouse

Journal of Environmental Chemical Engineering 10 (2022) 107807

https://doi.org/10.1016/j.jece.2022.107807

Higher performances of open vs. closed circuit microbial fuel cell sensor for nitrate monitoring in water

Zhenxing Ren [a,1], Guixia Ji [a], Hongbo Liu [a,*,1], Ping Li [b], Jianhong Huang [a], Eric Lichtfouse [c,2]

[a] School of Environment and Architecture, University of Shanghai for Science and Technology, 516 Jungong Road, 200093 Shanghai, China
[b] Chongqing New World Environment Detection Technology Co. LTD, 22 Jinyudadao, 401122 Chongqing, China
[c] Aix-Marseille Univ, CNRS, IRD, INRA, Coll France, CEREGE, 13100 Aix en Provence, France

ARTICLE INFO

Editor: Xianwei Liu

Keywords:
Nitrate monitoring
Open circuit
Sensitivity and stability
Response time
Microbial community

ABSTRACT

Microbial fuel cell (MFC) sensor exhibits attractive prospects for real-time monitoring of nitrate (NO_3^-) in water, with unique advantages of self-powering and simple structure; but its stability and sensitivity are unsatisfactory. In an attempt to address the limitations, here we employed an open-circuit MFC (O-MFC) sensor for real-time monitoring of NO_3^- in water, compared to a conventional closed-circuit MFC (C-MFC) sensor. The stability of the O-MFC sensor was confirmed when subject to the continuous fluctuation of interfering substances including organic matter (acetate, 2–20 mM), SO_4^{2-} (250–400 mg/L) and Fe^{3+} (0.3–0.6 mg/L). For one-time and continuous monitoring of NO_3^- at a concentration of 1–40 mg/L, the O-MFC sensor both achieved higher sensitivity than that of the C-MFC sensor; especially at a low NO_3^- concentration of 1 mg/L, the changes of electrical signal (ΔE) reached 10.0 ± 1.00 mV and 7.0 ± 0.85 mV respectively. In contrast, the C-MFC sensor failed to monitor at low NO_3^- concentrations of 1 and 5 mg/L. Moreover, good linear correlation between ΔE and NO_3^- concentration (R^2 = 0.907 and 0.981) was obtained from the O-MFC sensor. However, owing to the highly activity of EAB that mainly grows in the outer layer of biofilm, the response time of the O-MFC sensor is too long. Microbial community analysis further revealed that the open-circuit condition is more suitable for NO_3^- monitoring in water, providing a new way to improve the performance of MFC sensors.

1. Introduction

The increasing use of nitrates (NO_3^-) as crop fertilizers and the discharge of nitrate-rich wastewaters from municipal plants and livestock farms have induced eutrophication, hypoxia, acidification and changes in phytoplankton and microbial populations in water bodies, posing a serious threat to the ecosystem [1–3]. In addition, excessive nitrate in drinking water would cause serious healthy diseases, such as infant methemoglobinemia (blue baby syndrome), cancers, kidney disease and infertility [4,5]. Especially when nitrate is reduced to highly toxic nitrite by microorganisms, accumulated nitrite over than 3 g in the body could lead to death [6]. The world health organization (WHO) recommends a maximum concentration for NO_3^--N in drinking water resources of 10 mg/L [7]. Nitrate is a relatively stable anion and is not easily precipitated due to its high stability and solubility; it is necessary to monitor nitrate in time to avoid possible environmental and human health risks.

Some methods have been developed to quantify nitrate detection in water, such as ultraviolet spectrophotometry, fluorescence, ion exchange chromatography, cadmium column reduction and electrochemical analysis; among them, electrochemical methods have attracted increasing attention due to their portability, simplicity, economy and low detection limit [8–10]. The electrochemical methods for nitrate detection can be divided into voltammetric detection and potentiometric detection. Based on the difference in potential generated by selective passage of nitrate from a solution to a membrane, ion-selective electrodes (ISEs) is the most common potentiometric detection method with detection limits down to parts per trillion (ppt) level [10]. However, due to the electrode passivation and slow kinetics of direct nitrate reduction on electrode surface, ISEs have a poor sensitivity and a low reproducibility [11,12]. Over recent decades, the nitrate reductase (NR) biosensor based on the high levels of specificity and selectivity for

* Correspondence to: 516, Jungong Road, 200093 Shanghai, China.
E-mail address: Liuhb@usst.edu.cn (H. Liu).
[1] Zhenxing Ren and Hongbo Liu contribute equally to this work.
[2] Orcid: 0000-0002-8535-8073.

nitrate has attracted considerable interest, which exhibits ultra-high sensitivity and low detection limit [10,13]. With the development of different enzyme polymerization methods that load more NR per unit area, thereby enhancing the electron transfer process, NR biosensors can detect nitrate with low detection limits to 0.0076 μM NO_3^--N [14]. However, stability of NR biosensors is generally poor since it is susceptible to irreversible changes under the environmental factors and presence of toxicants [6]. In addition, it is difficult to maintain the detection repeatability of normal biosensors since NR has no self-regeneration ability and usually needs to be replaced and stored in a low-temperature environment, which makes it impossible to monitor nitrate in water continuously [15].

Alternatively, microbial fuel cell (MFC) sensors exhibit more attractive prospects for in-situ monitoring of nitrate in water, due to their unique advantages of self-powering, sustainable and good self-recovery ability [16,17]. The electroactive bacteria (EAB) of the bioanode as sensing element metabolically degrades the substrates and transports the electrons to the external circuit via extracellular electron transfer (EET) channels [18,19]. Since nitrate is a common electron acceptor of microbial metabolism, the presence of nitrate will compete for electrons with the outward EET, thereby changing the output current or voltage to a certain extent [20]. However, due to the competition between the microbial electricity generation and the denitrification processes, the sensitivity and accuracy of MFC sensors for nitrate detection is limited; the different C/N ratios in water significantly impact the competition on population dynamics in mixed communities and metabolic pathways [21]. Gregoire et al. revealed that some EAB are capable of bidirectional EET, i.e. organic oxidation by outward EET and nitrate reduction by inward EET, which avoid the nitrate competed with outward EET for electrons [22]. Yi et al. used the model electricigen *Shewanella loihica* PV-4 with the bidirectional EET capability simultaneously monitoring BOD and nitrate in water [23]. Considering the growth environment of pure bacteria in the actual monitoring scenario is easy to be contaminated, it is not conducive to long-term monitoring of nitrate in water with most MFC sensors [24]. Previous works indicated that lower electrode potential is thermodynamically feasible to improve the sensitivity of nitrate monitoring [25,26]. However, the electrode potential usually controlled by the potentiostat [27,28], which is in contradiction with the distinguished self-powered feature of MFC sensors. Yu et al. developed a MFC powered biocathode sensor to detect nitrate through dynamically controlled biocathode potential in the range of − 0.45 to − 0.7 V, and obtained a low detection limit (0.11 μM) and wide linear detection range (1–500 μM) [24]. To further simplify the construction of the MFC sensor and control the appropriate anode potential, Wang et al. employed an open-circuit MFC sensor cultured with mixed bacterial to monitor nitrate in water, and established a dynamic model of O-MFC sensor [29]. Since the open-circuit cuts off the path of electron transfer to the cathode, electrons can be stored in the cytochromes of microorganisms or electrode in the absence of electron acceptors, and the accumulation of electrons minimizes the anode potential [30]. Generally open-circuit MFC is not susceptible to organic matter [31]. However, due to the restricted electron transport path, which is not conducive to the growth and metabolism of EAB, the long-term open circuit of the MFC can easily lead to the deterioration of the bioanode [32]. When other interfering substances (such as Cu^{2+}, Fe^{3+} and Cr^{6+}) were present, the anodic microbial activity was inhibited under open-circuit conditions, leading to more obvious potential fluctuations [33]. The current generated under closed circuit condition is beneficial to stimulate the reactivation of the decaying anode biofilm [34].

In this study, an open-circuit MFC (O-MFC) sensor for real-time NO_3^- monitoring was constructed while another closed-circuit MFC (C-MFC) sensor constructed for comparison, in order to verify the superiority of open-circuit mode for nitrate monitoring in water. The effect of organic matter (OM, acetate) and other interfering ions (SO_4^{2-} and Fe^{3+}) on the stability of MFC sensors was investigated. Furthermore, the sensitivity and detection limit of the two sensors for real-time monitoring of NO_3^- in water were examined. After one month of continuous monitoring tests, the microbial community differences on their electrodes between the two MFC sensors were also explored.

2. Materials and methods

2.1. Construction and start-up of MFC sensors

Two typical dual chamber MFCs with the same configuration were constructed as NO_3^- detection sensors. The two chambers with each working volume of 50 ml were separated by a cation exchange membrane (CMI-7000, Membranes International Inc., USA). Graphite felt (2 × 3 × 0.2 cm) was used as anode, and the cathode was a carbon fiber brush (3 × φ1.5 cm). Ag/AgCl reference electrode (SCE, + 197 mV vs. SHE; CHI Co., Ltd., Shanghai, China) was placed in each of the anode chambers to measure the anode potential.

The operation conditions of two MFC sensors were identical during the start-up stage. The anode was connected to a potentiostat (CHI660E, CHI Co., Ltd., Shanghai, China) as the working electrode, and the cathode was used as the counter electrode. The anode potential was controlled at − 297 mV vs. Ag/AgCl reference electrode [35]. After the mixture replaced daily, the cell voltage of the MFCs was monitored for 3 h through the data acquisition board (Picolog1216, Pico Technology Inc, UK). The MFCs were inoculated with an anode mixture (1:3, V/V) of the inoculum and the synthetic wastewater. The inoculum was taken from the YE Wastewater Treatment Plant, Shanghai, and the synthetic wastewater was composed of 1.64 g NaAC, 0.31 g NH_4Cl, 4.40 g KH_2PO_4, 3.40 g K_2HPO_4, 0.10 g $CaCl_2{\cdot}H_2O$, 0.10 g $MgCl_2{\cdot}6H_2O$, 12.50 ml trace mineral solution and 5 ml vitamin solution dissolved in 1 L deionized water [36]. COD of the mixture solution was 740 ± 50 mg/L and pH was 6.65 ± 0.10. In order to remove dissolved oxygen, N_2 was used to purge the mixture solution for 20 min before injected to the anode chamber. The catholyte contained 16.64 g $K_3Fe(CN)_6$, 4.40 g KH_2PO_4 and 3.40 g $K_2HPO_4{\cdot}3H_2O$ in 1 L deionized water. Both the anolyte and catholyte were replaced daily. During the experiment, the temperature was controlled at 25 ± 2 °C. Magnetic stirrers were installed at the bottom of both chambers. The start-up stage was considered completed when the maximum voltage output of the MFCs is continuously stable for one week.

2.2. Test of the MFC sensors

After the start-up stage was completed, the anode chamber of MFCs were filled with synthetic wastewater to replace the mixture solution; both the anolyte and catholyte were recirculated at a flow rate of 5 ml/min and replaced every two days. One of the MFC sensor was operated under open-circuit condition which acted as the O-MFC sensor, and the other was connected to a 1000 Ω external resistor as the C-MFC sensor. The anode potential of the O-MFC sensor and external circuit voltage of the C-MFC sensor were recorded every 5 s by the data acquisition board (Fig. 1).

Once the MFC sensors reached steady states, a series of experiments were carried out to investigate performance variations of them. Firstly, the optimal background concentration of MFC sensors was determined under different acetate concentrations of 2 mM, 5 mM, 10 mM and 20 mM, respectively, which used as default value for all subsequent experiments, unless otherwise specified. Then, the effect of continuous changes of acetate concentration on the stability of the MFC sensors were investigated. Before a new concentration was applied, the electrical signal of sensors should return to steady-state and maintain for 30 min

In order to compare the performances (sensitivity, stability and response time) between the two MFC sensors for NO_3^- monitoring, two MFC sensors fed with synthetic wastewater containing different concentrations of NO_3^- (1 mg/L, 5 mg/L, 10 mg/L, 20 mg/L, 30 mg/L and

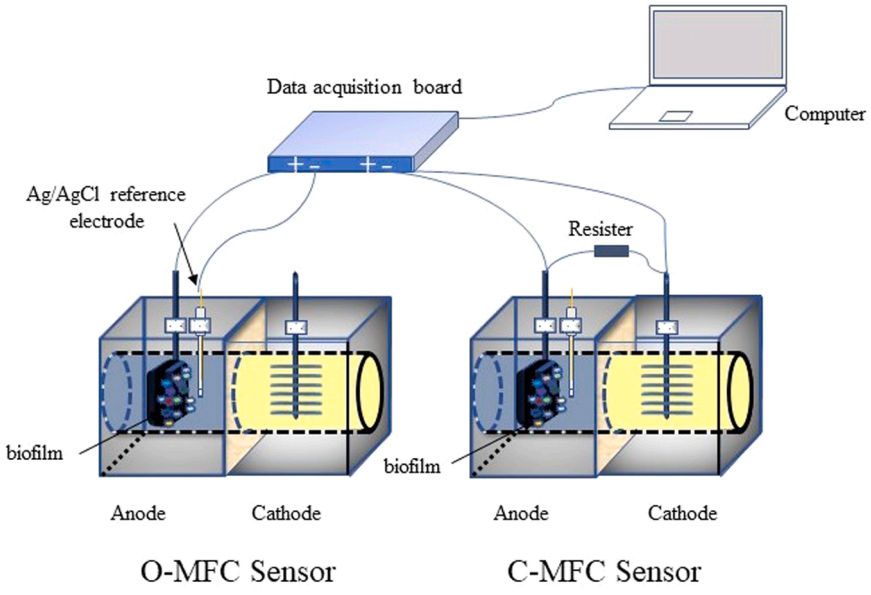

Fig. 1. Schematic diagram of O-MFC and C-MFC sensors.

40 mg/L) were tested. To simulate the actual working scenarios with complex condition changes, the one-time and continuous NO_3^- monitoring experiments were set for further investigations on the stability and repeatability of the MFC sensors. Considering that the response time of the MFC sensor previously reported was rather long [37], the experiments employed 30 min as the initial reaction time. For the one-time NO_3^- concentration monitoring experiments, the anode of sensors would be cleaned with 50 mM phosphate buffer solution (PBS) at the end of each operation run. For the continuous real time monitoring of NO_3^-, the voltage was retained at least 30 min for each run.

Afterwards, the effects of interfering ions (SO_4^{2-} and Fe^{3+}) acted as competing electron acceptances were investigated. For that 250 mg/L, 300 mg/L, 350 mg/L and 400 mg/L of SO_4^{2-} were passed into the anode chamber at a flow rate of 5 ml/min. Similarly, 0.3 mg/L, 0.4 mg/L, 0.5 mg/L and 0.6 mg/L of Fe^{3+} were tested with the same procedure as described above. The sensors were cleaned with 50 mM PBS after each experiment.

2.3. Analysis and calculations

Polarization and power density curves were obtained by linear sweep voltammetry (LSV), with the scan rate of 1 mV/s (CHI660E, CHI Co., Ltd., Shanghai, China), with the open-circuit potential and short-circuit potential as the initial potential and the final potential respectively. The results were obtained from the V-I curve. Cyclic voltammetry (CV) is used to characterize the redox behavior of bioanode, which was operated in a three-electrode mode with the scan potential ranging from − 0.8 to 0 V and the scan rate of 0.01 mV/s.

Response time was defined as the time required for the electrical signal (current or voltage) recovering to 95% of the initial steady-state signal after the MFC contacted with contaminants [20]. In this study, since the electrical signal generated was weak when subjected to shock of contaminants, the response time was defined as the time required to transit the electrical signal from one steady-state to another when subjected to shock of contaminants.

Sensitivity is an important parameter for MFC sensors and is generally defined as the change in electrical signal intensity (ΔE, mV) per unit concentration of the monitored substance (ΔC, mg/L) [20], as demonstrated in Eq. (1). In this study, since nitrate can also be metabolized by non-EAB, ΔE was used to represent the sensitivity of MFC sensors.

$$\text{Sensitivity} = \frac{\Delta E}{\Delta C} \tag{1}$$

Inhibition rate (IR) refers to the percentage of the changes in the electrical signal (ΔE, mV) to the initial value (U_0, mV) and is generally used to determine detrimental effect of toxic substance [20]. In this study, this index was used to evaluate the effect of interference substances on performances of the MFC sensors by Eq. (2).

$$\text{IR} = \frac{\Delta E}{U_0} \times 100\% \tag{2}$$

2.4. Anodic microbial community

After long time continuous monitoring tests for one month, the anode samples were cut under aseptic conditions and gently cleaned with 50 mmol/L PBS solution to remove the poorly adsorbed bacteria; then the electrodes were fixed with 2.5% (V/V) glutaraldehyde for 10 h. The fixed electrodes were cleaned with PBS solution six times for 20 min each time; after that, the electrodes were cleaned with 30%, 50%, 70%, 90% and 100% of ethanol by volume; each solution was soaked twice for 20 min. The treated electrode samples were vacuum dried, gold-mounted and observed under a JSM-6360LV scanning electron microscope.

The microbial diversity of the anodic biofilm was sequenced using an Illumina Miseq (Shanghai Majorbio Bio-pharm Technology Co., Ltd., China). The hypervariable regions were V3-V4, and corresponding primers were 338 F (50-ACTCCTACGGGAGGCAGCAG-30) and 806 R (50-GGACTACHVGGGTWTCTAAT-30) by the thermocycler PCR system (GeneAmp 9700, ABI, USA). Finally, the data was analyzed on the online platform of Majorbio I-Sanger Cloud Platform.

3. Results and discussion

3.1. Electrochemical characterization of MFC sensors after start-up

To evaluate background differences between the two MFC sensors after start-up, the CV, polarization and power density curves were profiled (start-up data were not given for streamlined content). The CV curve is an electrochemical technique used to characterize thermodynamics of electron transfer of EAB [38]. As shown in Fig. 2a, the oxidation and reduction peaks of MFCs both appeared at the formal

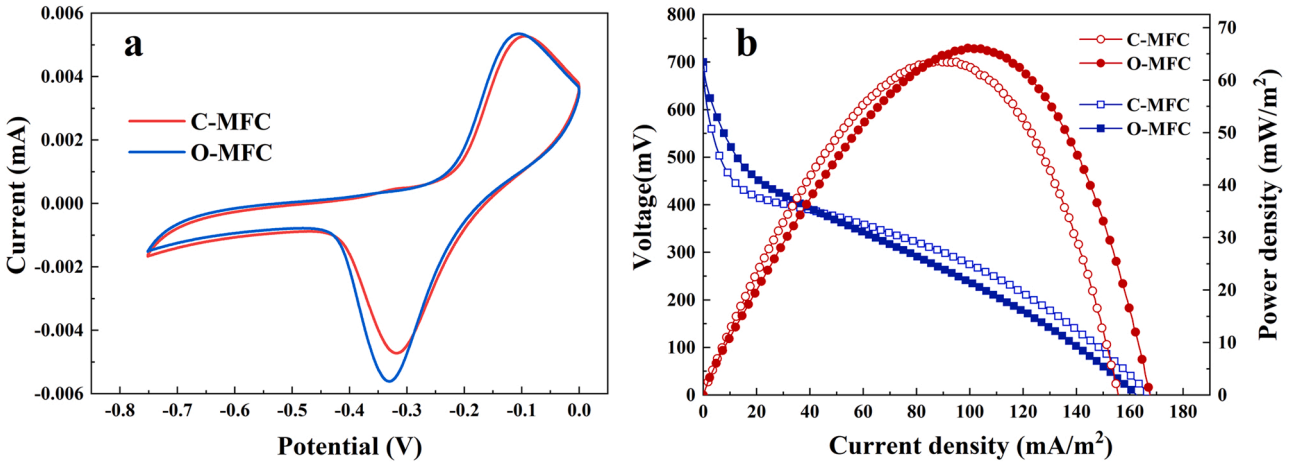

Fig. 2. **(a)** Cyclic voltammetry for enriched biofilms on anodes vs. Ag/AgCl for the two sensors; the scan potential ranging from − 0.8 to 0 V and the scan rate of 0.01 mV/s. **(b)** Polarization curves and power density curves of the two sensors after start-up; the scan rate of 1 mV/s.

potential around − 0.01 V and − 0.33 V, respectively. Although the Faradaic current of MFC-2 was slightly higher than that of MFC-1, the electroactive areas enclosed by the curves were close, which means that the thermodynamics, voltampere characteristics and anode electron transfer mechanism of MFC-1 and MFC-2 were similar [39]. As is illustrated in Fig. 2b, the similar open-circuit potential (around 700 mV) and the similar slop of cell polarization curves were observed for the two MFCs. The maximum power density achieved by the MFC-1 was 63.3 mW/m^2, which was only 1.8 mW/m^2 lower than that produced from the MFC-2. Besides, both MFCs obtained the same maximum current density around 163 mA/m^2. In summary, the bacterial metabolism and electroactivity on the bioanode of the two MFC sensors were similar, indicating that the differences between MFC-1 and MFC-2 were negligible, allowing for subsequent comparative experiments.

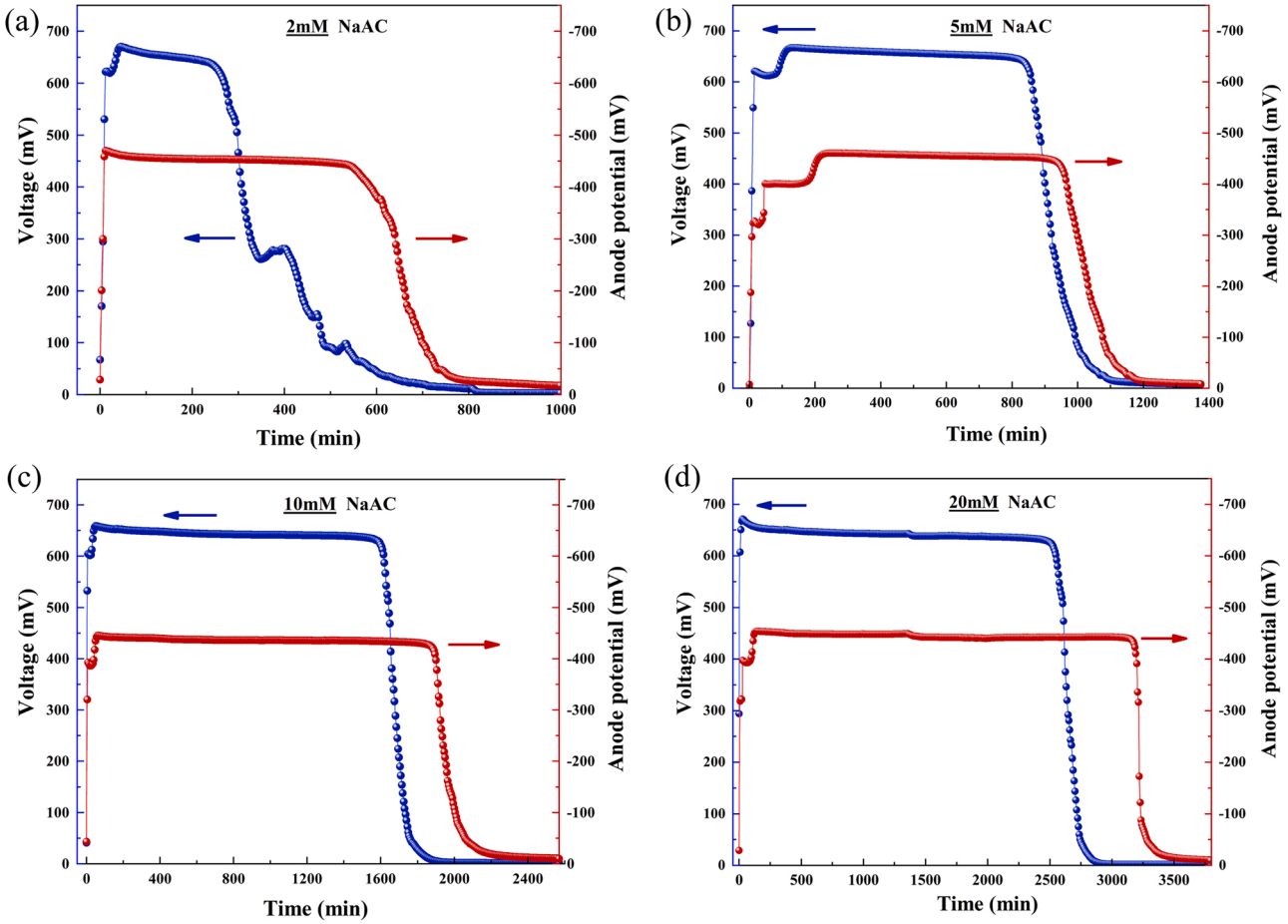

Fig. 3. The electrical signal of the sensors under different acetate concentrations of 2 mM **(a)**, 5 mM **(b)**, 10 mM **(c)** and 20 mM **(d)** respectively.

3.2. Effects of organic matter (OM in water on performances of MFC sensors

To estimate the optimal background concentration of OM, the effect of acetate at 2–20 mM had been investigated (Fig. 3). Results showed that the electrical signal of both MFC sensors reached maximum values in a short time, with about − 450 mV and 650 mV for the O-MFC and the C-MFC sensor, respectively. As shown in Fig. 3a, a steady-state anode potential was observed from the O-MFC sensor maintaining for about 450 min at 2 mM of acetate dosage. In contrast, the voltage of the C-MFC sensor decreased slowly after reaching the maximum value and started to drop sharply after about 280 min, implying that the OM concentration of 2 mM is insufficient for the tests. Besides, significant voltage fluctuation appeared during the voltage drop process of the C-MFC sensor after 280 min, which was caused by the complex microbial interaction and diverse metabolism in mixed culture [40], indicating a more intense electrons competition relationship in closed-circuit mode. Electrical signal of MFC sensors subject to 5–20 mM of acetate showed a longer plateau time and the steady-state time increased with acetate concentrations (Fig. 3b–d). In particular, the steady-state times of the C-MFC and O-MFC sensors were up to 1787 min, 3012 min and 1520 min, 2330 min at 10 mM and 20 mM OM, respectively. Previous studies have shown that excessive organic concentration was not conducive to nitrate monitoring and easily leads to false negatives [41, 42]. Therefore, the optimal background concentration of OM was identified as 5 mM.

The effect of continuous fluctuations of the acetate concentration on the response of sensors was tested (Fig. S1). Results showed that changing acetate concentrations from 2 to 10 mM then from 10 to 20 mM had little effect on the anode potential of the O-MFC sensor; the ΔE produced by the acetate change were 2 ± 0.51 mV, 3 ± 0.44 mV, and 3 ± 0.38 mV, respectively; the response time gradually increased with the increase of acetate concentration, with the longest time about 32 min; the steady-state signal was maintained at about − 450 mV with small fluctuation. Nevertheless, significant voltage fluctuations were observed from investigations of the C-MFC sensor. When the influent water with an OM concentration of 2 mM passed into the C-MFC sensor, the voltage dropped from 638 mV to 632 mV and maintained for 30 min due to insufficient substrates. With the increase of OM concentration to 10 mM, the voltage returned to 638 mV and remained steadily, which was complied with the role of OM degradation and electron transfer. Surprisingly, the voltage began to drop dramatically while the OM increased to 20 mM, which may be due to the predominance of *Aceto-clastic methanogenesis* over the activity of the EAB, thereby reduced the voltage output [43]. In addition, the voltage of the closed-circuit sensor was controlled by the external resistance and cathode receptor, thus it was more prone to change. This fluctuation for OM further revealed that the closed-circuit sensor lacks stability of performance. In contrast, the anode potential of the O-MFC sensor was mainly related to the charging current generated by the oxidation of OM. When the anode capacitance is certain and the electron saturation is in the steady state, the capacitance depended on the content of cytochrome C on the anode biofilm [29,44]. From this prospect, the O-MFC sensor had higher stability when the OM concentration fluctuates in the range of 2–20 mM in water, thus it was more conducive to NO_3^- monitoring in aquatic environment containing organic matters.

3.3. Performances of one-time NO_3^- monitoring tests

Detection range of the MFC sensors was assessed by varying NO_3^- levels from 1 to 40 mg/L (details were listed in Table 1). As illustrated in Fig. 4a, the O-MFC sensor showed a high sensitivity of 10.0 ± 1.0 mV at 1 mg/L NO_3^- and a short response time of 10.0 ± 4.5 min. Meanwhile, the detection concentration of 1 mg/L NO_3^- was lower than the detection limit of previous studies based on the same type of MFC sensors [29,33], which was one-tenth of the upper limit for NO_3^- concentration specified in the drinking water standard [45]. Although the C-MFC sensor also showed a voltage drop at 1 mg/L NO_3^-, the voltage lost stability could not return to the steady-state in a long time. The same problem was found when the NO_3^- concentration was 5 mg/L (Fig. 4b); but the problem was eliminated when the NO_3^- concentration was greater than 10 mg/L (Fig. 4c–f), suggesting that the detection limit of the C-MFC sensor is 10 mg/L. The distinct ΔE of the O-MFC sensor were observed at NO_3^- concentrations of 5–40 mg/L. However, the increase of ΔE was much smaller than that of the NO_3^- concentration and the response time of both sensors increased significantly, indicating that the reduction efficiency of NO_3^- receiving electrons on the bioanode surface was inversely proportional to its concentration. Since the denitrifying non-EAB proliferated on the anode, reduced the NO_3^- but didn't consume electrons from the anode, the lower ΔE produced by higher NO_3^- concentration at 30 and 40 mg/L NO_3^-. The correlation between NO_3^- concentration and ΔE of the MFC sensors was shown in Fig. S2. Since the C-MFC sensor failed to detect NO_3^- at low concentrations of 1 mg/L and 5 mg/L, only 4 points were fitted using logarithm based on their distribution. There was no significant linear correlation between ΔE and NO_3^- concentration in the C-MFC sensor (Fig. S2a). However, such linear relationship was evident in the O-MFC sensors with the R^2 of 0.907 (Fig. S2b), which indicated that the open-circuit was more suitable for NO_3^- quantification tests. These results implied that the O-MFC sensor used for one-time NO_3^- monitoring tests presented a wider monitoring range (1–40 mg/L), greater stability and higher sensitivity.

Table 1
Performances of two MFC sensors for one-time NO_3^- monitoring.

Nitrate concentration (mg/L)	C-MFC sensor		O-MFC sensor	
	Sensitivity (mV)	Response time (min)	Sensitivity (mV)	Response time (min)
1	/	/	10.0 ± 1.5	10.0 ± 4.5
5	/	/	22.0 ± 2.4	14.0 ± 5.6
10	11.0 ± 1.2	19.0 ± 3.6	27.0 ± 2.8	21.0 ± 7.5
20	12.0 ± 2.4	33.0 ± 8.9	29.0 ± 2.5	41.0 ± 9.9
30	18.0 ± 3.7	69.0 ± 9.0	30.0 ± 3.5	66.0 ± 9.8
40	16.0 ± 2.1	52.0 ± 9.4	27.0 ± 3.4	63.0 ± 9.5

/: not available.

3.4. Performance of continuous NO_3^- monitoring in water

Prominent differences of the response time, sensitivity and detection limit in continuous monitoring of NO_3^- concentrations ranging from 1 to 40 mg/L were demonstrated in Table 2. Likewise, the C-MFC sensor was unable to generate significant ΔE to detect low-concentration nitrates at 1 mg/L and 5 mg/L (Fig. 5a). When a higher NO_3^- concentration was applied, the steady-state signal of the C-MFC sensor dropped from the initial 651 to 645 mV, which might be caused by the accumulation effect of nitrate that promoted the growth of non-electrogenic bacteria on surface of the bioanode, and competed for OM with the EAB. Compared with the one-time monitoring tests, the ΔE generated under the same nitrate concentration (10–40 mg/L) was lower in the continuous tests. This might be attributed to the reduction of EAB abundance in anodic colony and the thickening of biofilm. Due to the accumulation of NO_3^-, the activity of EAB was inhibited and thus the response time of the O-MFC sensor at the corresponding concentration was longer than that of the one-time monitoring tests. As can be seen from Fig. 5b, the linear correlation ($R^2 = 0.587$) between the NO_3^- concentration and the ΔE for the C-MFC sensor was low, but it provided a reference for early warning of the NO_3^- pollution in water within a certain range (10–40 mg/L).

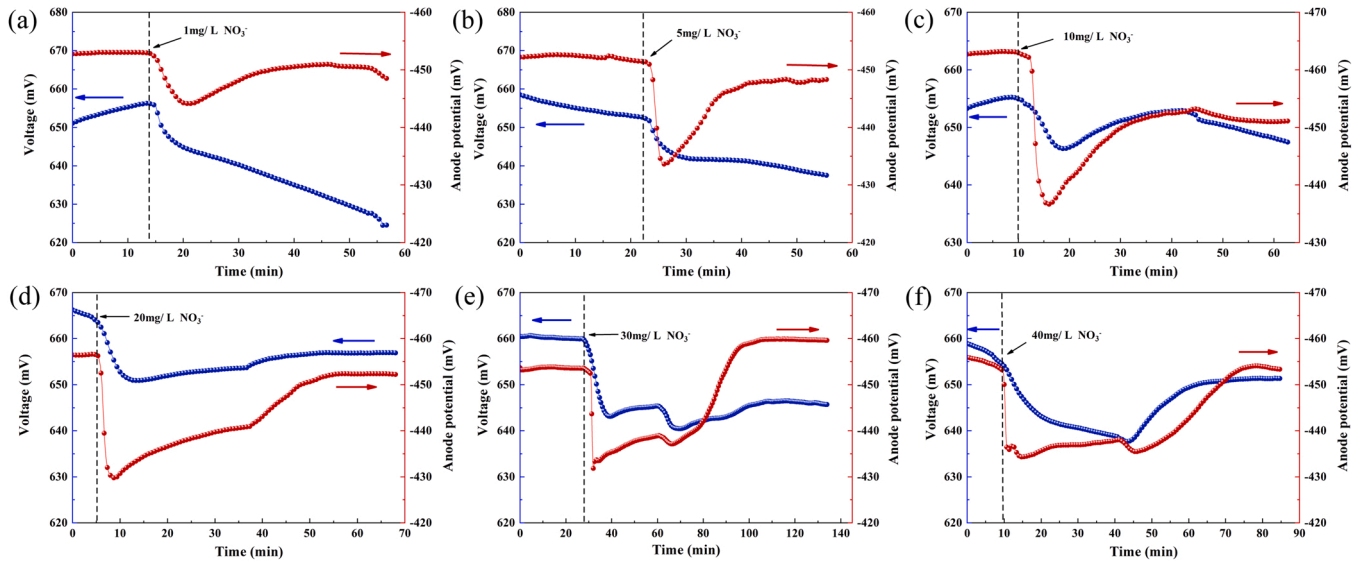

Fig. 4. The electrical signal of the O-MFC and C-MFC sensors subject to different NO_3^- concentrations of 1 mg/L **(a)**, 5 mg/L **(b)**, 10 mg/L **(c)**, 20 mg/L **(d)**, 30 mg/L **(e)** and 40 mg/L **(f)** respectively.

Table 2
Performance of two MFC sensors for continuous NO_3^- monitoring.

Nitrate concentration (mg/L)	C-MFC sensor		O-MFC sensor	
	Sensitivity (mV)	Response time (min)	Sensitivity (mV)	Response time (min)
1	/	/	7.0 ± 1.2	17.0 ± 4.4
5	/	/	19.0 ± 2.3	29.0 ± 3.4
10	3.0 ± 1.7	40.0 ± 4.2	22.0 ± 1.7	61.0 ± 5.7
20	5.0 ± 1.5	41.0 ± 6.1	25.0 ± 1.2	123.0 ± 5.3
30	6.0 ± 1.7	66.0 ± 7.5	26.0 ± 1.6	137.0 ± 7.5
40	5.0 ± 1.1	80.0 ± 5.3	27.0 ± 1.5	262.0 ± 8.4

/: not available.

In comparison, when the O-MFC sensor was used for continuous monitoring of NO_3^- in water with the concentration range of 1–40 mg/L, the higher sensitivity and better stability were shown in Fig. 5c. The fast responses of anode potential were observed at different nitrate concentrations due to the open-circuit conditions that pose a higher electron competitive advantage to nitrate. The potential responses under different nitrate concentrations are similar to those of one-time monitoring tests (Table 2), indicating that the O-MFC sensor has better robustness and repeatability. It is noteworthy that despite the increasing nitrate concentration, the steady-state signal of the O-MFC sensor was hardly affected by the accumulation effect of nitrate and recovered to the initial value easily (around − 455 mV). To some extent, it showed that the bioanode of O-MFC sensor had the stationary charge capacity which was consistent with previous studies [29]. However, the response time of O-MFC sensor was too long, which prevents its application. After the anode potential reacheed the highest value, the anode potential gradually recovers and the nitrate reduction process continues to consume electrons, but the consumption rate was less than the generation rate of electrons. The electron yield was directly related to the number and community structure of anode EAB, which requires further analysis of anode microbial community. In Fig. 5d, the ΔE and the NO_3^- concentration exhibited a good linear relationship in the concentration range of 1–40 mg/L ($R^2 = 0.981$), indicated that the open-circuit MFC sensor had great development potential for the real time quantitative monitoring of NO_3^-. Based on performances of the C-MFC and O-MFC sensors for continuous monitoring of NO_3^-, the O-MFC sensor had more advantages in terms of sensitivity, detection limit, stability and liner correlation, but the long response time was a challenge of the proposed approach for real-time monitoring.

3.5. *Interference of SO_4^{2-} and Fe^{3+} on performances of the MFC sensors*

SO_4^{2-} is one of the most abundant anions in nature water that has similar properties of NO_3^- and is commonly used as an electron acceptor. The upper limit for SO_4^{2-} concentration specified in the drinking water standard is 250 mg/L [46]. Interference of SO_4^{2-} on electrical signal of MFC sensors was illustrated in Fig. 6a, with the concentrations varying from 250 mg/L to 400 mg/L. Compared with the C-MFC sensor, smaller fluctuations in electrical signal of the O-MFC sensor were obtained when the SO_4^{2-} concentration was 250 mg/L, 300 mg/L, 350 mg/L and 400 mg/L in order, and corresponding voltage fluctuations were 1.00 ± 0.52 mV, 1.00 ± 0.41 mV, 1.00 ± 0.56 mV and 2.00 ± 0.43 mV respectively (Table S3). When the interference SO_4^{2-} reached up to 400 mg/L, the highest IR of the C-MFC sensor was only 0.92 ± 0.27% with a small output voltage fluctuation. These results showed that the competition ability of microorganisms getting electrons from SO_4^{2-} was limited for the reason that the anodic potentials of MFC sensors (O-MFC: − 450 mV, C-MFC: − 384 mV) were not low enough to reduce SO_4^{2-}, whose reduction potential is − 700 mV vs. Ag/AgCl [47]. As shown in Fig. 6b, higher stability was demonstrated for the O-MFC sensor when it was exposed to Fe^{3+} interference with concentrations of 0.3 mg/L, 0.4 mg/L, 0.5 mg/L and 0.6 mg/L; the corresponding ΔE were 0.50 ± 0.02 mV, 0.50 ± 0.10 mV, 1.50 ± 0.12 mV, and 0.60 ± 0.15 mV respectively, indicating that the addition of Fe^{3+} had almost no impact on performances of the O-MFC sensor. In contrast, the impact of Fe^{3+} interference on performances of the C-MF sensor was sluggish and continuous. When subject to 0.3 mg/L of Fe^{3+} interference, the output voltage started to drop slowly and continuously. This drop-trend was distinguished from other toxic substances such as Cu^{2+} and Cd^{2+} that had a milder inhibitory effect on the activity of EAB and inactivated a fraction of EAB but most of them survived, which is consistent with the findings of other researchers [33]. Overall, the interfering ions of SO_4^{2-} and Fe^{3+} widely present in water bodies had little impact on monitoring stability of the O-MFC sensor.

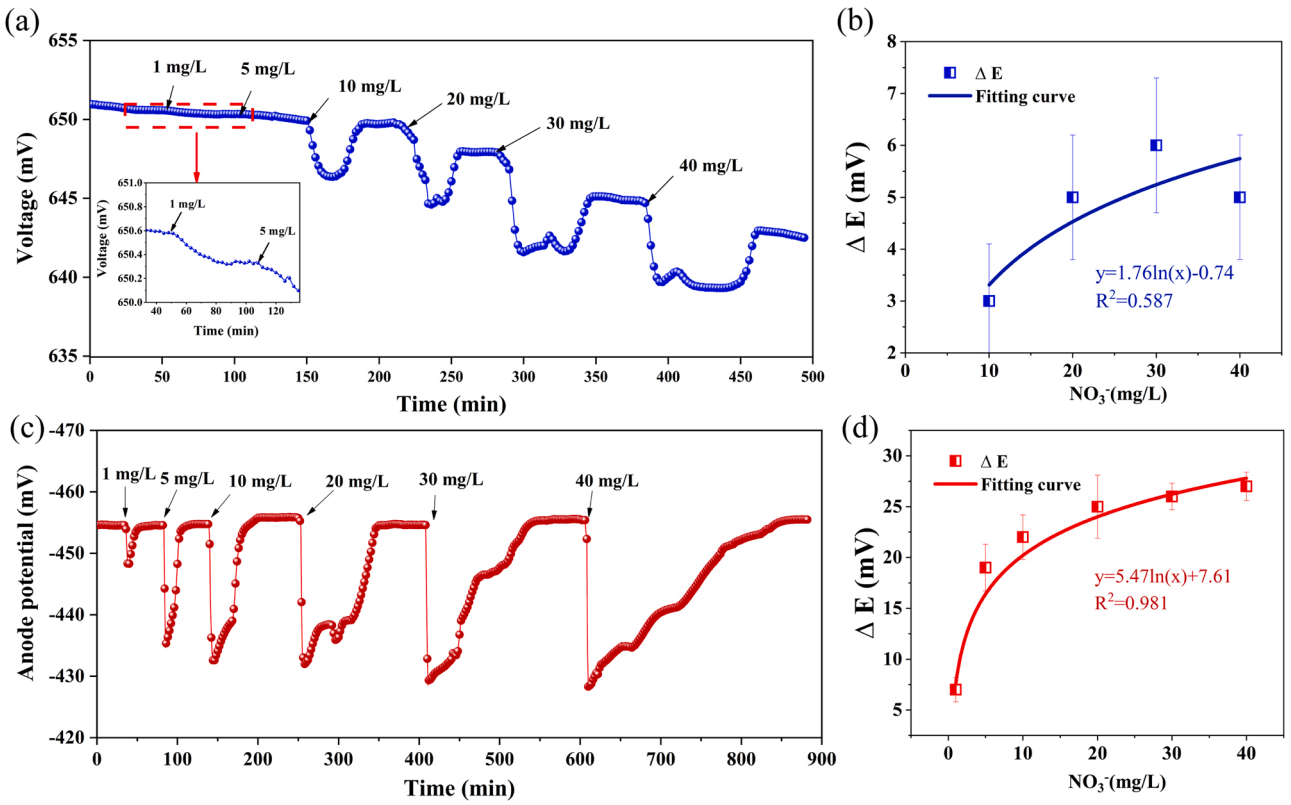

Fig. 5. The electrical signal of the C-MFC sensor **(a)** and the O-MFC sensor **(c)** for continuous NO_3^- detection, with corresponding the correlation between the NO_3^- concentration and ΔE of the C-MFC sensor **(b)** and O-MFC sensor **(d).**

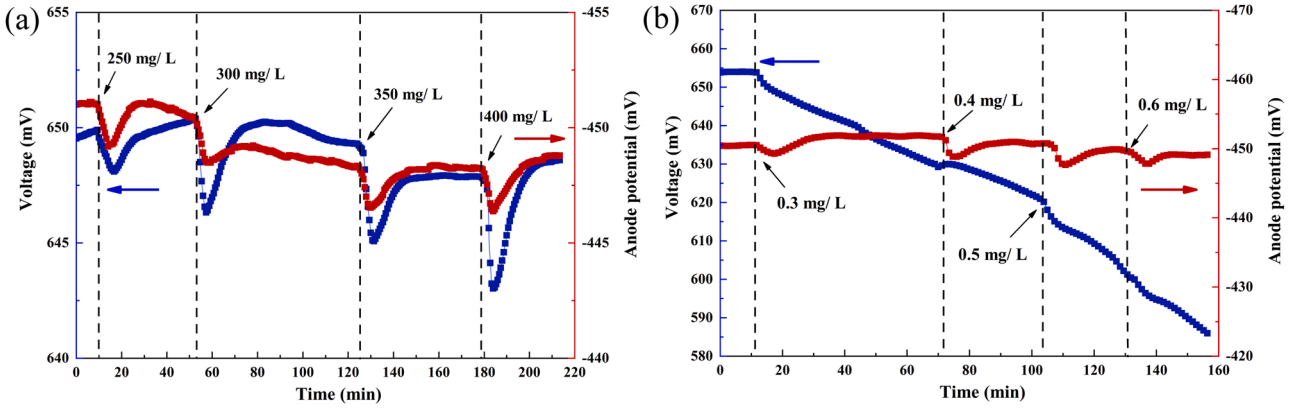

Fig. 6. Effects of interference substances SO_4^{2-} **(a)** and Fe^{3+} **(b)** on performances of the two MFC sensors.

3.6. Role of anode microbial communities

SEM images revealed the topographic features on electrodes surface after one month of continuously monitoring tests. As shown in Fig. 7a, part of the graphite felt was completely wrapped by bacteria on bio-anode surface of the C-MFC sensor. Biofilm development on the graphite felt was beneficial to microbial electricity generation, but the electron transfer resistance would increase and lower the NO_3^- reduction rate when the biofilm was too dense. In comparison, a looser bacteria distribution was obtained on the O-MFC sensor anode surface (Fig. 7b), which would be more conducive to communication and electron transfer of microorganisms.

To explore differences between the sensors after a month of continuous monitoring, the composition and abundance of microbial communities in the phylum and genus levels were retrieved in Table 3. The difference in the genus structure of the microbial community was more significant than that in the phylum structure. *Proteobacteria* and *Bacteroidota* were the major components at the phylum level for both sensors, with a total proportion of at least 70%. Known EAB classified to the phylum of *Proteobacteria*, such as *Geobacter sulfurreducens* [48], *Shewanella oneidensis* [49], *Rhodopseudomonas* [50] and *Comamonas* [48], are critical for sensors to generate bioelectricity and maintain voltage stability. In the genus level, *Chorobaculum* was the unique genera in the C-MFC sensor system compared with the O-MFC sensor system, with the highest abundance of 30.0% (Fig. 7c). *Chlorobaculum* is a strictly anaerobic photoautotrophic microorganism and uses sulfide as electrons donor to produce monomeric sulfur that is deposited outside the cell [51]. It is generally considered that *Chorobaculum* is an unfavorable indicator for microbial electricity generation and denitrification [52]. The massive growth of *Chorobaculum* can explain the low sensitivity of

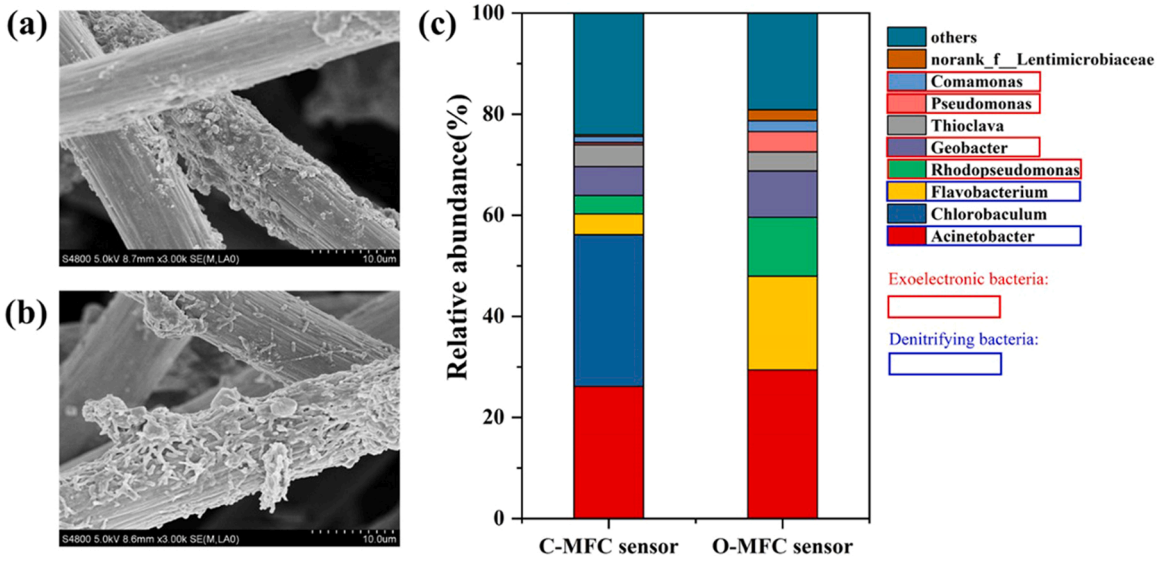

Fig. 7. The SEM of anodes surface from the C-MFC (a) and O-MFC (b) sensors after one month of continuously monitoring tests; (c) composition of bacterial communities at the genus level for both MFC sensors.

Table 3
The dominant phylum and genera of the two MFC sensors with the corresponding relative abundance.

Taxonomy		Relative abundance (%)	
Phyla	Genera	C-MFC sensor (%)	O-MFC sensor (%)
Proteobacteria	*Acinetobacter*	26.14	29.39
	Rhodopseudomonas	3.64	11.65
	Thioclava	4.30	3.81
	Pseudomonas	0.43	4.02
	Comamonas	1.23	2.12
Bacteroidota	*Chlorobaculum*	30.01	0.01
	Flavobacterium	4.12	18.55
	norank_f_Lentimicrobiaceae	0.33	2.19
Desulfobacterota	*Geobacter*	5.72	9.14
	others	24.06	19.13

the C-MFC sensor in nitrate monitoring. In the O-MFC sensor system, *Acinetobacter* was the most dominant genus (29.39%), which is a group of bacteria with multiple catabolic capacity for a large number of organic matter [53]. Through break down complex organic matter into simpler ones that are then consumed by the EAB, it can promote more efficient electron production. The total proportion of EAB in O-MFC sensor was 26.93% and higher than that in C-MFC sensor (11.02%), including *Geobacter* (9.14%), *Rhodopseudomonas* (11.65%), *Pseudomonas* (4.02%) and *Comamonas* (2.12%). Theoretically, high abundance EAB is beneficial to shorten the recovery time of MFC sensor after being impacted by nitrate, but the previous results showed that the recovery time of O-MFC sensor was longer than C-MFC sensor. This might be due to the limited extracellular electron transfer caused by the distribution of EAB on the anode surface, which affects the recovery of anode potential. Previous studies have shown that highly active EABs mainly grows in the outer layer of biofilm under open-circuit conditions [32]. The total abundance of denitrifying bacteria in the O-MFC system (47.94%) was also higher than that in the C-MFC system (30.26%). Denitrifying bacteria such as *Acinetobacter* and *Flavobacterium* were obtained on both two sensors, which can accelerate the effective electron transfer for nitrate reduction and electricity generation, it is vital to NO_3^- detection in water [54]. The groups of functional microorganisms and their relative abundances on electrode surface determined performance of the MFC sensors. The results confirmed that the O-MFC sensor was more suitable for the formation of electrogenic and denitrifying bacteria in the system, which explained that the O-MFC sensor has higher sensitivity and lower detection limit from the microbial level.

4. Conclusions

The comparative evaluation of the two MFC sensors indicated that the O-MFC sensor had more promising application prospect for real-time monitoring of NO_3^- in water. Compared to the conventional C-MFC sensor, the sensitivity and detection range of the O-MFC sensor for NO_3^- monitoring in water had been effectively improved. Meanwhile, ΔE of the O-MFC sensor showed a good liner correlation at the NO_3^- concentration of 1–40 mg/L, which implied good development potential for the quantitative detection and analysis of NO_3^- in water. The anode potential of the O-MFC sensor was almost unaffected under the interference of different substances including OM, SO_4^{2-} and Fe^{3+}, indicating that it was more suitable for nitrate monitoring in natural water environment with complicated quality conditions. After one month of continuous monitoring tests, the abundance of EAB (26.93%) and denitrifying bacteria (47.94%) on anode surface of the O-MFC sensor were higher than that of the C-MFC sensor (11.02% and 30.26% respectively), providing a long-term validity for the O-MFC sensor.

CRediT authorship contribution statement

Zhenxing Ren: Investigation and part of the draft manuscript, Methodology, mechanism modeling. **Guixia Ji:** Investigation, Supervision. **Hongbo Liu:** Funding acquisition, Conceptualization and part of the draft manuscript, Project administration, Supervision. **Ping Li:** Data curation. **Jianhong Huang:** Investigation, Methodology. **Eric Lichtfouse:** Writing – review & editing.

Declaration of Competing Interest

The authors declare that they have no known competing financial interests or personal relationships that could have appeared to influence the work reported in this paper.

Acknowledgements

We gratefully acknowledged the co-funding of this work by the National Natural Science Foundation of China (No. 52070130) and the

Shuguang Project of Shanghai (Education and Scientific Research Project of Shanghai, 18SG45).

Appendix A. Supporting information

Supplementary data associated with this article can be found in the online version at doi:10.1016/j.jece.2022.107807 and below.

References

[1] S.E. Vollset, E. Goren, C.-W. Yuan, J. Cao, A.E. Smith, T. Hsiao, C. Bisignano, G. S. Azhar, E. Castro, J. Chalek, et al., Fertility, mortality, migration, and population scenarios for 195 countries and territories from 2017 to 2100: a forecasting analysis for the Global Burden of Disease Study, Lancet 396 (2020) 1285–1306, https://doi.org/10.1016/s0140-6736(20)30677-2.

[2] Y. Teng, R. Zuo, Y. Xiong, J. Wu, Y. Zhai, J. Su, Risk assessment framework for nitrate contamination in groundwater for regional management, Sci. Total Environ. 697 (2019), 134102, https://doi.org/10.1016/j.scitotenv.2019.134102.

[3] B. Zhang, Y. Jiang, K. Zuo, C. He, Y. Dai, Z.J. Ren, Microbial vanadate and nitrate reductions coupled with anaerobic methane oxidation in groundwater, J. Hazard. Mater. 382 (2020), 121228, https://doi.org/10.1016/j.jhazmat.2019.121228.

[4] M. Šrajbek, L. Kranjčević, I. Kovač, R. Biondić, Groundwater nitrate pollution sources assessment for contaminated wellfield, Water 14 (2022) 255.

[5] S. Bijay, E. Craswell, Fertilizers and nitrate pollution of surface and ground water: an increasingly pervasive global problem, SN Appl. Sci. 3 (2021), https://doi.org/10.1007/s42452-021-04521-8.

[6] Z. Lin, S. Cheng, H. Li, L. Li, A novel, rapidly preparable and easily maintainable biocathode electrochemical biosensor for the continuous and stable detection of nitrite in water, Sci. Total Environ. 806 (2022), https://doi.org/10.1016/j.scitotenv.2021.150945.

[7] D. Su, Y. Chen, Advanced bioelectrochemical system for nitrogen removal in wastewater, Chemosphere 292 (2022), 133206, https://doi.org/10.1016/j.chemosphere.2021.133206.

[8] Q.-H. Wang, L.-J. Yu, Y. Liu, L. Lin, R.-g. Lu, J.-p. Zhu, L. He, Z.-L. Lu, Methods for the detection and determination of nitrite and nitrate: a review, Talanta 165 (2017) 709–720, https://doi.org/10.1016/j.talanta.2016.12.044.

[9] C. Jiang, Y. He, Y. Liu, Recent advances in sensors for electrochemical analysis of nitrate in food and environmental matrices, Analyst 145 (2020) 5400–5413, https://doi.org/10.1039/d0an00823k.

[10] M. Sohail, S.B. Adeloju, Nitrate biosensors and biological methods for nitrate determination, Talanta 153 (2016) 83–98, https://doi.org/10.1016/j.talanta.2016.03.002.

[11] M. Sharma Shelly, Fabrication of enzyme nanoparticles-based nanosensor for detection of nitrate content in drinking water, Asian J. Pharmaceut. 14 (2020) 133–138.

[12] T. Kalaria, H. Gill, S. Harris, C. Ford, R. Gama, The effect of haemolysis on the direct and indirect ion selective electrode measurement of sodium, Ann. Clin. Biochem. 58 (2020) 190–195, https://doi.org/10.1177/0004563220987593.

[13] J. Moore, Microbial biosensors: a review, J. Microb. Biochem. Technol. 13 (2021).

[14] S.-G. Woo, S.-J. Moon, S.K. Kim, T.H. Kim, H.S. Lim, G.-H. Yeon, B.H. Sung, C.-H. Lee, S.-G. Lee, J.H. Hwang, et al., A designed whole-cell biosensor for live diagnosis of gut inflammation through nitrate sensing, Biosens. Bioelectron. 168 (2020), 112523, https://doi.org/10.1016/j.bios.2020.112523.

[15] T. Monteiro, S. Gomes, E. Jubete, L. Añorga, C.M. Silveira, M.G. Almeida, A quasi-reagentless point-of-care test for nitrite and unaffected by oxygen and cyanide, Sci. Rep. 9 (2019) 2622, https://doi.org/10.1038/s41598-019-39209-y.

[16] M.H. Do, H.H. Ngo, W. Guo, S.W. Chang, D.D. Nguyen, Y. Liu, S. Varjani, M. Kumar, Microbial fuel cell-based biosensor for online monitoring wastewater quality: a critical review, Sci. Total Environ. 712 (2020), 135612, https://doi.org/10.1016/j.scitotenv.2019.135612.

[17] H.J. Yang, M.H. Zhou, M.M. Liu, W.L. Yang, T.Y. Gu, Microbial fuel cells for biosensor applications, Biotechnol. Lett. 37 (2015) 2357–2364.

[18] Z. Wang, B. Zhang, Y. Jiang, Y. Li, C. He, Spontaneous thallium (I) oxidation with electricity generation in single-chamber microbial fuel cells, Appl. Energy 209 (2018) 33–42, https://doi.org/10.1016/j.apenergy.2017.10.075.

[19] C. Zhong, B. Zhang, L. Kong, A. Xue, J. Ni, Electricity generation from molasses wastewater by an anaerobic baffled stacking microbial fuel cell, J. Chem. Technol. Biotechnol. 86 (2011) 406–413, https://doi.org/10.1002/jctb.2531.

[20] Y. Jiang, X. Yang, P. Liang, P. Liu, X. Huang, Microbial fuel cell sensors for water quality early warning systems: fundamentals, signal resolution, optimization and future challenges, Renew. Sustain. Energy Rev. 81 (2018) 292–305, https://doi.org/10.1016/j.rser.2017.06.099.

[21] F. Zhang, Z. He, Integrated organic and nitrogen removal with electricity generation in a tubular dual-cathode microbial fuel cell, Process Biochem. 47 (2012) 2146–2151, https://doi.org/10.1016/j.procbio.2012.08.002.

[22] K.P. Gregoire, S.M. Glaven, J. Hervey, B. Lin, L.M. Tender, Enrichment of a high-current density denitrifying microbial biocathode, J. Electrochem. Soc. 161 (2014) H3049–H3057, https://doi.org/10.1149/2.0101413jes.

[23] Y. Yi, T. Zhao, B. Xie, Y. Zang, H. Liu, Dual detection of biochemical oxygen demand and nitrate in water based on bidirectional Shewanella loihica electron transfer, Bioresour. Technol. 309 (2020), 123402, https://doi.org/10.1016/j.biortech.2020.123402.

[24] Y.Y. Yu, X.L. Ding, W.Z. Quan, Q.J. Niu, Z. Fang, M.F. Dapaah, T.Y. You, X. Xiao, L. Cheng, Dynamically controlling the electrode potential of a microbial fuel cell-powered biocathode for sensitive quantification of nitrate, Electrochim. Acta 369 (2021), https://doi.org/10.1016/j.electacta.2020.137661.

[25] L. Zhang, J. Ong, J. Liu, S.F.Y. Li, Enzymatic electrosynthesis of formate from CO_2 reduction in a hybrid biofuel cell system, Renew. Energy 108 (2017) 581–588, https://doi.org/10.1016/j.renene.2017.03.009.

[26] X. Qi, S. Wang, T. Li, X. Wang, Y. Jiang, Y. Zhou, X. Zhou, X. Huang, P. Liang, An electroactive biofilm-based biosensor for water safety: pollutants detection and early-warning, Biosens. Bioelectron. 173 (2020), 112822, https://doi.org/10.1016/j.bios.2020.112822.

[27] Y. Yang, Y.-Y. Yu, Y.-T. Shi, J.M. Moradian, Y.-C. Yong, In vivo two-way redox cycling system for independent duplexed electrochemical signal amplification, Anal. Chem. 91 (2019) 4939–4942, https://doi.org/10.1021/acs.analchem.9b00053.

[28] Y. Jiang, P. Liang, P.P. Liu, D.L. Wang, B. Miao, X. Huang, A novel microbial fuel cell sensor with biocathode sensing element, Biosens. Bioelectron. 94 (2017) 344–350, https://doi.org/10.1016/j.bios.2017.02.052.

[29] D. Wang, P. Liang, Y. Jiang, P. Liu, B. Miao, W. Hao, X. Huang, Open external circuit for microbial fuel cell sensor to monitor the nitrate in aquatic environment, Biosens. Bioelectron. 111 (2018) 97–101, https://doi.org/10.1016/j.bios.2018.04.018.

[30] A. Esteve-Núñez, J. Sosnik, P. Visconti, D.R. Lovley, Fluorescent properties of c-type cytochromes reveal their potential role as an extracytoplasmic electron sink in Geobacter sulfurreducens, Environ. Microbiol. 10 (2008) 497–505, https://doi.org/10.1111/j.1462-2920.2007.01470.x.

[31] G. Pasternak, J. Greenman, I. Ieropoulos, Self-powered, autonomous biological oxygen demand biosensor for online water quality monitoring, Sens. Actuators B: Chem. 244 (2017) 815–822, https://doi.org/10.1016/j.snb.2017.01.019.

[32] X. Zhang, A. Prévoteau, R.O. Louro, C.M. Paquete, K. Rabaey, Periodic polarization of electroactive biofilms increases current density and charge carriers concentration while modifying biofilm structure, Biosens. Bioelectron. 121 (2018) 183–191, https://doi.org/10.1016/j.bios.2018.08.045.

[33] B. Liu, Y. Lei, B. Li, A batch-mode cube microbial fuel cell based "shock" biosensor for wastewater quality monitoring, Biosens. Bioelectron. 62 (2014) 308–314, https://doi.org/10.1016/j.bios.2014.06.051.

[34] J. Yu, Y. Park, T. Lee, Electron flux and microbial community in microbial fuel cells (open-circuit and closed-circuit modes) and fermentation, J. Ind. Microbiol. Biotechnol. 42 (2015) 979–983, https://doi.org/10.1007/s10295-015-1629-2.

[35] T.Y. Chou, C.G. Whiteley, D.-J. Lee, Q. Liao, Control of dual-chambered microbial fuel cell by anodic potential: implications with sulfate reducing bacteria, Int. J. Hydrog. Energy 38 (2013) 15580–15589, https://doi.org/10.1016/j.ijhydene.2013.04.074.

[36] X. Wang, N. Gao, Q. Zhou, Concentration responses of toxicity sensor with Shewanella oneidensis MR-1 growing in bioelectrochemical systems, Biosens. Bioelectron. 43 (2013) 264–267, https://doi.org/10.1016/j.bios.2012.12.029.

[37] H. Kashima, J.M. Regan, Facultative nitrate reduction by electrode-respiring geobacter metallireducens biofilms as a competitive reaction to electrode reduction in a bioelectrochemical system, Environ. Sci. Technol. 49 (2015) 3195–3202, https://doi.org/10.1021/es504882f.

[38] F. Guo, H. Liu, Impact of heterotrophic denitrification on BOD detection of the nitrate-containing wastewater using microbial fuel cell-based biosensors, Chem. Eng. J. 394 (2020), 125042, https://doi.org/10.1016/j.cej.2020.125042.

[39] Y.P. Zhang, J. Sun, B. Hou, Y.Y. Hu, Performance improvement of air-cathode single-chamber microbial fuel cell using a mesoporous carbon modified anode, J. Power Sources 196 (2011) 7458–7464, https://doi.org/10.1016/j.jpowsour.2011.05.004.

[40] V.N. Srinivasan, C.S. Butler, Ecological and transcriptional responses of anode-respiring communities to nitrate in a microbial fuel cell, Environ. Sci. Technol. 51 (2017) 5334–5342, https://doi.org/10.1021/acs.est.6b06572.

[41] L. Peixoto, B. Min, G. Martins, A.G. Brito, P. Kroff, P. Parpot, I. Angelidaki, R. Nogueira, In situ microbial fuel cell-based biosensor for organic carbon, Bioelectrochemistry 81 (2011) 99–103, https://doi.org/10.1016/j.bioelechem.2011.02.002.

[42] J. Davis, M.J. Moorcroft, S.J. Wilkins, R.G. Compton, M.F. Cardosi, Electrochemical detection of nitrate and nitrite at a copper modified electrode, Analyst 125 (2000) 737–742, https://doi.org/10.1039/a909762g.

[43] T.H.J.A. Sleutels, L. Darus, H.V.M. Hamelers, C.J.N. Buisman, Effect of operational parameters on Coulombic efficiency in bioelectrochemical systems, Bioresour. Technol. 102 (2011) 11172–11176, https://doi.org/10.1016/j.biortech.2011.09.078.

[44] G.D. Schrott, P.S. Bonanni, J.P. Busalmen, Open circuit potentiometry reports on internal redox states of cells in G. Sulfurreducens biofilms, Electrochim. Acta 303 (2019) 176–182, https://doi.org/10.1016/j.electacta.2019.02.078.

[45] K.M. Lockhart, A.M. King, T. Harter, Identifying sources of groundwater nitrate contamination in a large alluvial groundwater basin with highly diversified intensive agricultural production, J. Contam. Hydrol. 151 (2013) 140–154, https://doi.org/10.1016/j.jconhyd.2013.05.008.

[46] M. Coma, S. Puig, N. Pous, M.D. Balaguer, J. Colprim, Biocatalysed sulphate removal in a BES cathode, Bioresour. Technol. 130 (2013) 218–223, https://doi.org/10.1016/j.biortech.2012.12.050.

[47] J. Rakoczy, S. Feisthauer, K. Wasmund, P. Bombach, T.R. Neu, C. Vogt, H. H. Richnow, Benzene and sulfide removal from groundwater treated in a microbial fuel cell, Biotechnol. Bioeng. 110 (2013) 3104–3113, https://doi.org/10.1002/bit.24979.

[48] J.N. Li, Y.L. Yu, D.H. Chen, G.H. Liu, D.Y. Li, H.S. Lee, Y.J. Feng, Hydrophilic graphene aerogel anodes enhance the performance of microbial electrochemical systems, Bioresour. Technol. 304 (2020), https://doi.org/10.1016/j.biortech.2020.122907.
[49] J.C. Biffinger, J.N. Byrd, B.L. Dudley, B.R. Ringeisen, Oxygen exposure promotes fuel diversity for Shewanella oneidensis microbial fuel cells, Biosens. Bioelectron. 23 (2008) 820–826, https://doi.org/10.1016/j.bios.2007.08.021.
[50] D. Xing, Y. Zuo, S. Cheng, J.M. Regan, B.E. Logan, Electricity generation by Rhodopseudomonas palustris DX-1, Environ. Sci. Technol. 42 (2008) 4146–4151, https://doi.org/10.1021/es800312v.
[51] H. Yan, M.D. Yates, J.M. Regan, Effects of constant or dynamic low anode potentials on microbial community development in bioelectrochemical systems, Appl. Microbiol. Biotechnol. 99 (2015) 9319–9329, https://doi.org/10.1007/s00253-015-6907-4.
[52] Z. Zeng, Y.T. Fu, D.Y. Guo, Y.X. Wu, O.E. Ajayi, Q.F. Wu, Bacterial endosymbiont Cardinium cSfur genome sequence provides insights for understanding the symbiotic relationship in Sogatella furcifera host, Bmc Genom. 19 (2018), https://doi.org/10.1186/s12864-018-5078-y.
[53] Q. Zhang, L. Zhang, H. Wang, Q. Jiang, X. Zhu, Simultaneous efficient removal of oxyfluorfen with electricity generation in a microbial fuel cell and its microbial community analysis, Bioresour. Technol. 250 (2018) 658–665, https://doi.org/10.1016/j.biortech.2017.11.091.
[54] A. Al-Mamun, M.S. Baawain, Accumulation of intermediate denitrifying compounds inhibiting biological denitrification on cathode in microbial fuel cell, J. Environ. Health Sci. 13 (2015).

Supplementary material

Higher performances of open versus closed circuit microbial fuel cell sensor for nitrate monitoring in water

Zhenxing Ren[1a], Guixia Ji[a], Hongbo Liu[1*a], Ping Li[b], Jianhong Huang[a], Eric Lichtfouse[c]

a School of Environment and Architecture, University of Shanghai for Science and Technology, 516 Jungong Road, 200093, Shanghai, China. b Chongqing New World Environment Detection Technology Co.LTD, 22 Jinyudadao, 401122, Chongqing, China. c Aix-Marseille Univ, CNRS, IRD, INRA, Coll France, CEREGE, 13100 Aix en Provence, France. Orcid: 0000-0002-8535-8073

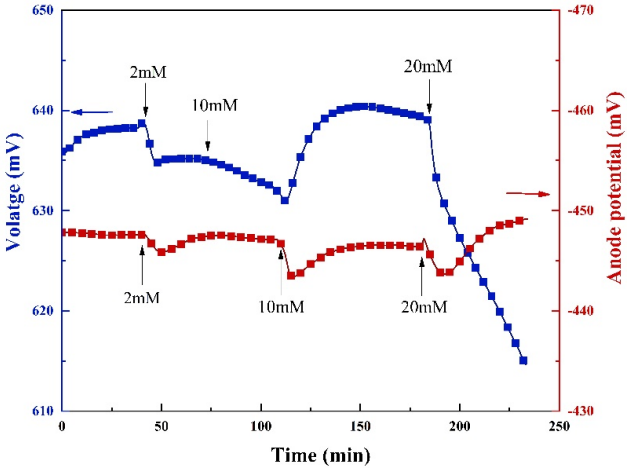

Fig. S1. The electric signal of the MFC sensors applying continuous variation acetate

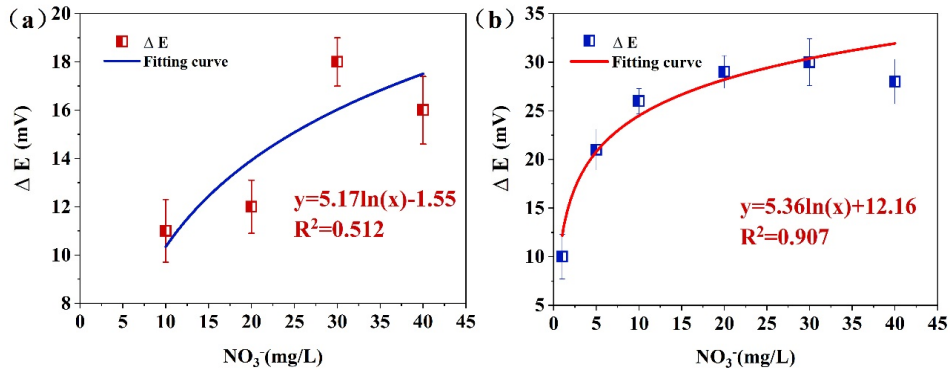

Fig. S2. The relationship between NO_3^- concentration and ΔE of the MFC sensors

* Corresponding author ADD: 516, Jungong Road, 200093, Shanghai, China;

Email: Liuhb@usst.edu.cn (H., Liu) Tel: +86(21)55275979; Fax: +86(21)55275979

1 Zhenxing Ren and Hongbo Liu contribute equally to this work

Table S1. Voltage drops and IR of the MFC biosensors under interference of SO_4^{2-} and Fe^{3+} in water.

Interfering substances	Concentration (mg/L)	Δ E (mV)	O-MFC sensor IR (%)	Δ E (mV)	C-MFCsensor IR (%)
SO_4^{2-}	250	1.00±0.52	0.22±0.12	2.00±0.44	0.31±0.14
	300	1.00±0.41	0.22±0.09	4.00±0.43	0.62±0.17
	350	1.00±0.56	0.22±0.15	5.00±0.32	0.77±0.33
	400	2.00±0.43	0.44±0.11	6.00±0.55	0.92±0.27
Fe^{3+}	0.3	0.50±0.02	0.11±0.18	/	/
	0.4	0.50±0.10	0.11±0.13	/	/
	0.5	1.50±0.12	0.33±0.12	/	/
	0.6	0.60±0.15	0.13±0.21	/	/

/: not available